Construction and Building Materials 141 (2017) 343–352

Contents lists available at ScienceDirect

Construction and Building Materials

journal homepage: www.elsevier.com/locate/conbuildmat

Assessment of Greener Cement by employing thermally treated sugarcane straw ashes

Eduardo Gurzoni Alvares Ferreira [a], Fabiano Yokaichiya [c], Michelle S. Rodrigues [b], Antonio L. Beraldo [b], Augusta Isaac [d], Nikolay Kardjilov [c], Margareth K.K.D. Franco [a,*]

[a] Instituto de Pesquisas Energéticas e Nucleares–IPEN–Reator Multipropósito Brasileiro – RMB, Brazil
[b] Universidade Estadual de Campinas (UNICAMP), Faculdade de Engenharia Agrícola (FEAGRI), Campinas, SP, Brazil
[c] Helmholtz-Zentrum Berlin fürMaterialienund Energie – HZB, Germany
[d] Universidade Federal de Minas Gerais, Department of Metallurgical and Materials Engineering, Belo Horizonte, MG, Brazil

HIGHLIGHTS

- Sugarcane straw ashes (SCSA) are suitable as pozzolanic material for cement uses.
- A Rietveld refinement method using C-S-H phase was successfully done.
- The cement setting time was delayed by SCSA burned at 700 °C.
- SCSA burned at different temperatures shows pores with different size and form.
- Replace 20% of clinker by SCSA is a good option to recover agroindustrial wastes.

ARTICLE INFO

Article history:
Received 21 July 2016
Received in revised form 24 February 2017
Accepted 4 March 2017
Available online 11 March 2017

Keywords:
Synchrotron radiation
Characterization
Sugarcane straw ash
Pozzolan
Waste management

ABSTRACT

Sustainable development has been growing concern worldwide, with special emphasis to its effects on climate change. An important action to reduce the environmental damage is the decrease of cement use. In this study the pozzolanicity of Sugarcane Straw Ashes (SCSA), thermal treated, at different curing times was investigated. Synchrotron X-ray Powder Diffraction measurements allowed the quantification of several phases of the cement pasts through Rietveld analysis. The properties of cement paste are directly related to the concentrations of Alite, Belite, Portlandite, Brownmilite and amorphous phases. Tomography technique was also used to study the differences amongst the pore structures according to type of ash used. The SCSA substitution of 20% (weight) in Ordinary Portland Cement (OPC) shows to be a good option to recover the agroindustrial wastes.

1. Introduction

The cement industry is facing unprecedented challenges related to depleting of fossil fuels and growing environmental concerns linked to climate change [1]. The most widely used form of that material today – Portland cement – is made by heating limestone and clay in kilns in a process that sends nearly a tonne of CO_2 skywards for a similar amount of final product. The manufacture of Portland cement accounts for roughly 5% of all man-made greenhouse gas emissions [2].

Nonetheless, the prospect of carbon taxes and cap-and-trade markets has led several industry groups to embrace green or sustainable cement alternatives.

A remarkable contribution towards a sustainable development of the cement and concrete industries can be achieved by a partial replacement of cement with pozzolans, a broad class of siliceous materials that reacts chemically with calcium hydroxide in the presence of water at ordinary temperature to form compounds with cementitious properties.

The general definition of a pozzolans includes a large number of materials which vary widely in terms of origin, composition and properties. Major sources of natural and artificial pozzolans include volcanic mineral deposits, fired and crushed clay, and furnace slag from industrial processes such manufacturing steel

* Corresponding author.
E-mail address: margareth_franco@yahoo.com.br (M.K.K.D. Franco).

http://dx.doi.org/10.1016/j.conbuildmat.2017.03.022
0950-0618/

[3]. The benefits of using pozzolanic material as additive or partial substitute to cement are basically threefold: first, the process emits less CO_2 and requires less energy, second, the economic gain obtained by replacing a substantial part of the cement by cheap and abundant materials and, third, to offer the opportunity to create value by converting industrial by products into durable construction materials [4–8].

Sugarcane straw ashes (SCSA) are a by-product of sugarcane which can be used as a pozzolan to substitute the cement [4,6,7]. In Brazil, millions of tons of sugarcane are produced every year. Each ton generates about 20 kg of ash, becoming an environment liability that this industry has to deal it. Currently, although is not appropriate, the ashes are being used as fertilizer.

Significant progress in green cement technology has been made over the last years [4–10]. However, further improvements in the cement formulation and production are contingent on deeper understanding of its structural and chemical features as well as its pozzolanic activity [11–13]. Here, we investigate the behavior of green cements during the hydration processes by synchrotron X-ray diffraction and computed microtomography, providing original and valuable information that is not accessible by other techniques. We report the impact of the calcining temperature on sugarcane straw ashes (SCSA) which were used as partial substitute to Portland cement, demonstrating the potentially of this approach in answering questions about its structure and composition and the reactions that ensue when it is mixed with water.

Table 1
Chemical composition and LOI of SCSAs at various conditions.

T_{calc} [°C]	LOI	Composition [%]										
		SiO_2	Al_2O_3	Fe_2O_3	TiO_2	CaO	MgO	Na_2O	SO_3	P_2O_5	Cl	K_2O
600	2.97	64.4	9.29	3.93	1.19	3.83	2.54	0.07	3.29	2.00	0.68	5.44
700	2.08	61.0	9.2	4.99	1.29	4.40	2.79	0.15	3.85	2.29	0.55	6.98
800	1.74	62.3	8.55	4.57	1.14	5.24	2.7	0.14	4.3	2.2	0.17	6.42
900	0.89	64.7	9.62	4.54	1.21	4.11	2.79	0.16	2.64	2.5	0.06	5.37

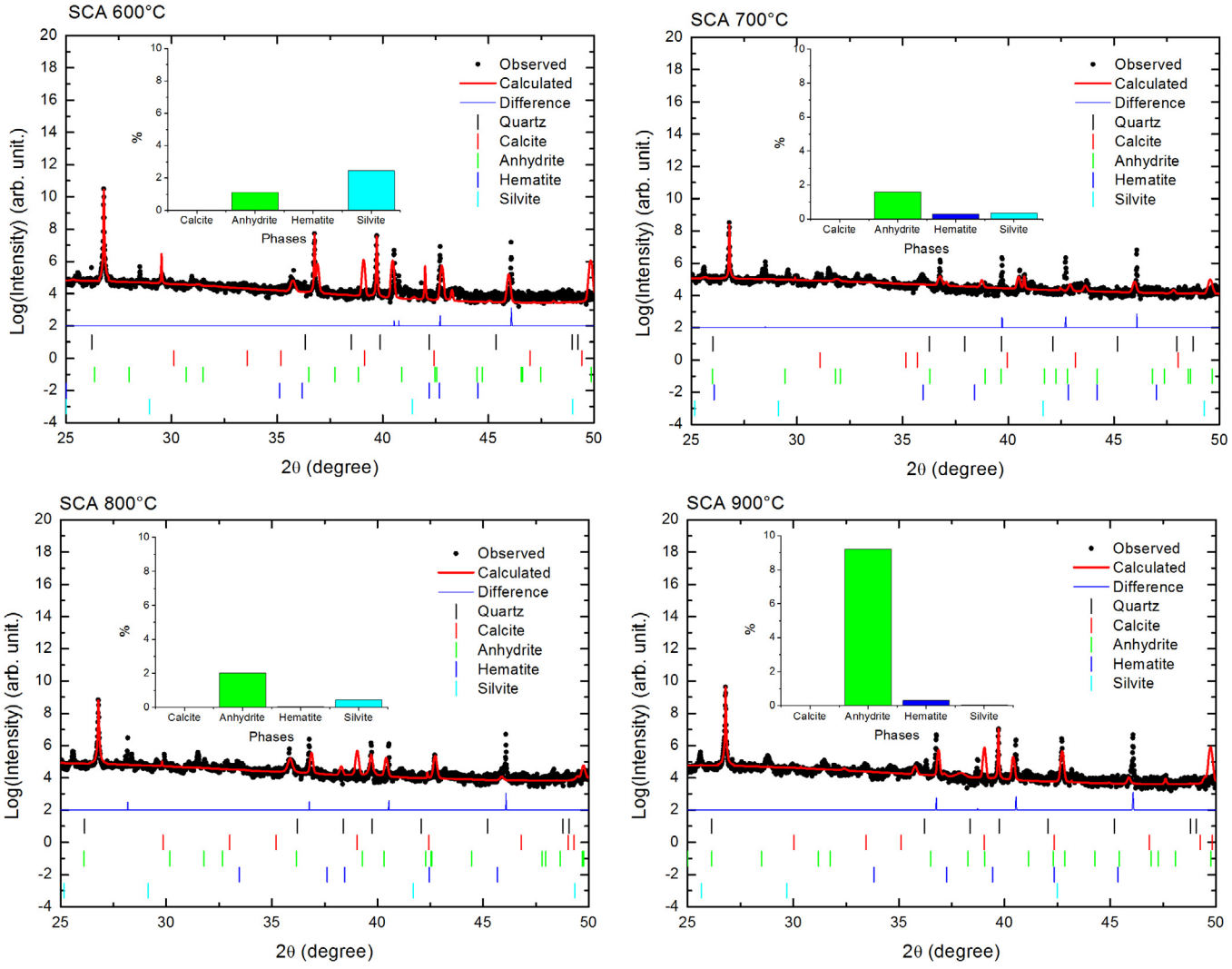

Fig. 1. XRD pattern of the SCSA-600 (a), SCSA-700 (b), SCSA-800 (c) and SCSA-900 (d).

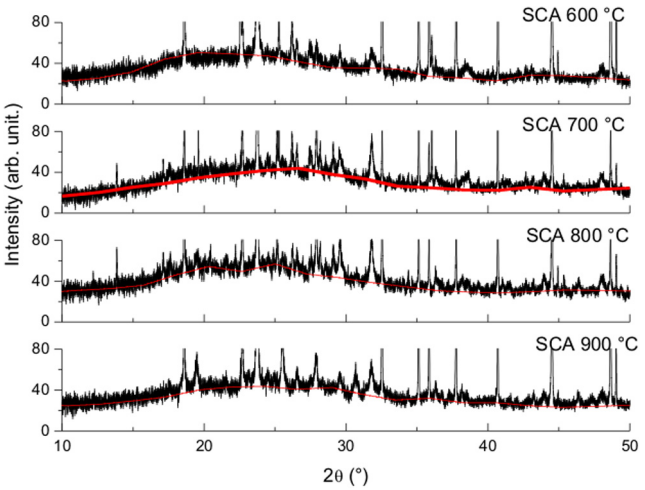

Fig. 2. XRD patterns of the SCSA-600, SCSA-700, SCSA-800 and SCSA-900 samples.

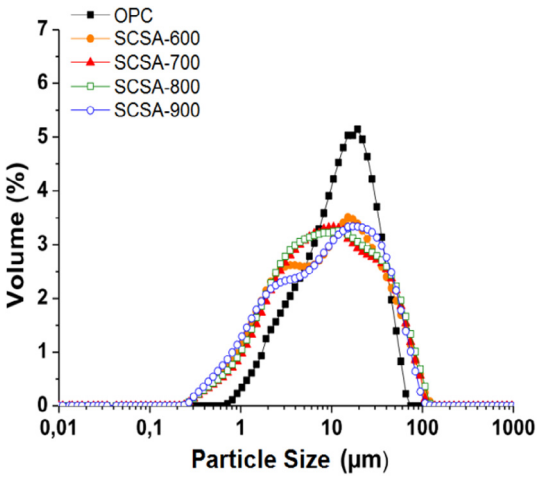

Fig. 3. Particle distribution size of the SCSA and OPC.

Table 2
Equivalent diameter of the particles after grinding.

Ashes	D 10 (μm)	D 50 (μm)	D 90 (μm)	Average Diameter (μm)
SCSA-600	1.39	9.63	45.81	17.44
SCSA-700	1.55	9.02	47.00	17.40
SCSA-800	1.47	8.51	43.81	16.33
SCSA-900	1.26	9.80	45.00	17.21

Notes: D10, D50, and D90 stands for those ash particles diameters below which the accumulated percentage is 10%, 50%, and 90%, respectively.

2. Experimental procedure

2.1. Materials

2.1.1. Sugarcane straw ashes

Sugarcane straws, composed of dried and fresh leaves as well as top of the plant, were provided by Centro de Tecnologia Canavieira (CTC), located in Piracicaba, São Paulo, Brazil. Prior to preparation of the combustion ashes, the sugarcane straws were air dried for 24 h, and divided in four batches. Thereafter, sugarcane straw ashes (SCSA) were obtained from the combustion of those materials at different calcining temperatures.

In order to ensure a homogenous burning, all batches were first heated at a rate of 10 °C/min till a temperature of 400 °C, and kept at this temperature for 20 min. Then, each batch were obtained through a specific temperature, i.e. 600, 700, 800, and 900 °C, for one hour. The electric furnace was turned off and the samples were let cool down inside. After cooling, the ashes were milled using a rotor mill at 200 rpm for 120 min prior to the analyses.

2.1.2. Green cements

Ordinary Portland Cement (OPC) finely ground with no mineral additions was used in this study, resulting in a cement with more reactivity (High Early Strength Cement, CPV-ARI, Cauê, according to the ABNT NBR 5733 [14]). Cement paste specimens were made with a water/binder ratio of 0.5.

Distinct types of green cements were produced by partially replacing the cement CPV-ARI with 20 wt% sugarcane straw ashes (SCASs) burned at different temperatures. Blended specimens were cast mixing the OPC cement with the natural pozzolans, and then adding deionized water. The specimens were cast in plastic bottles and immediately sealed. The curing process occurred at 20 °C, being interrupted after 7, 28, and 90 days using acetone. All samples were, then, dried at 60 °C for 30 min in common furnace in order to remove acetone.

2.2. Materials characterization

2.2.1. Chemical, structural, and physical properties of SCSAs

Chemical analysis of the SCSAs burned at different calcining temperatures was conducted to determine the effectiveness of these materials in contributing to sulfate resistance using X-ray fluorescence spectrometer (RX Axios Advance, PANalytical, Phillips spectrometer). The carbon content was determined by loss on ignition (LOI), according to ASTM C 114 standard [15].

In addition, information on the phases present in the samples and their crystallinity degree was assessed by X-ray diffraction (XRD) using synchrotron radiation, which is recognized as a well-established technique that had many advantages over the conventional diffractometer. Using a large photon flux of a synchrotron source is possible to evaluate the mineralogical composition of

Table 3
Phase description of the SCSA/OPC pastes components.

Phase	Formulae	Nomenclature	Crystal System Notation
Alite [22]	C_3SiO_5	C_3S	M1-Monoclinic Pc(7) M3-Monoclinic Cm(8)
Belite [23]	C_2SiO_4	C_2S	Monoclinic P $12_1/c1$(14)
Portlandite [24]	$Ca(OH)_2$	CH	Trigonal P -3*m*
Ettringite [25]	$Ca_6Al_2(SO_4)_3(OH)_{12}{\cdot}26H_2O$	AFt	Trigonal P31c
Calcite [26]	$CaCO_3$	$CaCO_3$	Trigonal R-3c
Brownmillerite [27]	$Ca_2(Al,Fe)_2O_5$	C4AF	Orthorrombic Pcmn(62)
Periclase [28]	MgO	MgO	Isometric Fm3m
Quartz [29]	SiO_2	SiO_2	Trigonal P *32 2 1*

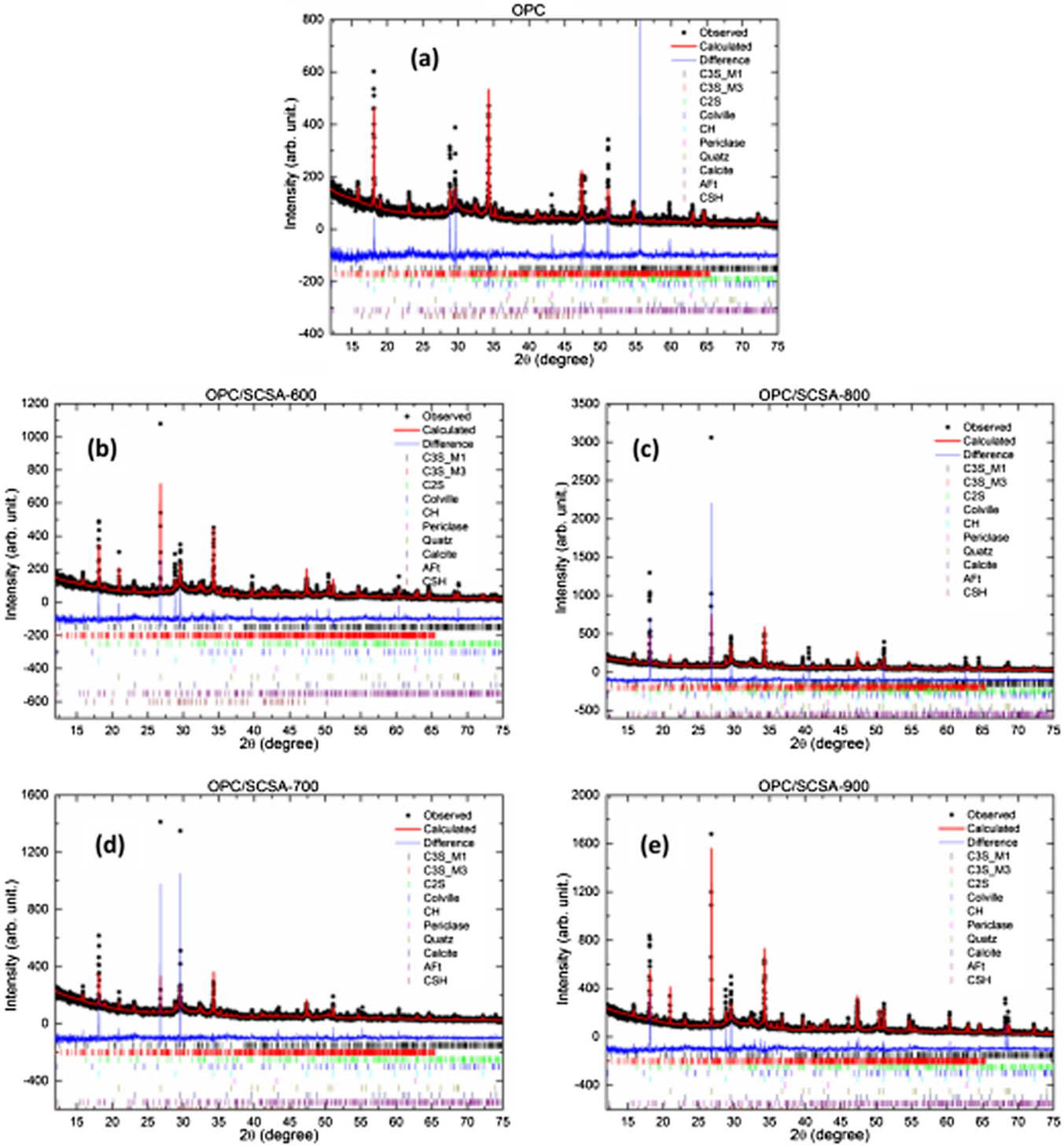

Fig. 4. Diffraction patterns of OPC (a), OPC/SCSA-600 (b), OPC/SCSA-700 (c), OPC/SCSA-800 (d), and OPC/SCSA-900 (e), cured for seven days.

materials with higher angular resolution, more accuracy, and in a shorter time, when compared with conventional XRD [19,20]. The experiments were performed at the X-ray powder diffraction beamlines D10B-XPD [16,17] at the synchrotron light source LNLS, in Campinas, Brazil. The measurements were carried out using a 4 + 2 circles Huber diffractometer in high resolution mode (with Ge 111 analyzer crystal) at 8 keV. The data acquisition was performed in a θ-2θ geometry over a 2θ range of 10°–70° with a step rate of 0.01° per second, with a flat plane sample holder.

The particle size distribution was determined using a laser diffractometer Mastersizer 2000 (Malvern Instruments, England). This analyzer is designed for measuring particle sizes between 0.02 and 2000 μm. The samples were dispersed in a suitable liquid media. The measurements started with the setup of laser obscuration values between 10 and 15% and ultrasonic agitation for 60 s [18].

2.2.2. Chemical, structural, and morphological properties of green cements

In order to investigate the effect of calcining temperature and curing time on the pozzolanic activation of SCSA-OPC mixtures, synchrotron XRD and X-ray microtomography techniques were

Table 4
Rietveld reliability factors and GOF for all analyzed samples.

Sample	R_{wp}	R_{exp}	GOF (R_{wp}/R_{exp})
OPC 7 days	18,287	6,613	2,765
OPC 28 days	15,874	6,131	2,589
OPC 90 days	18,680	14,243	1,312
OPC/SCSA 600 °C 7 days	17,220	11,958	1,440
OPC/SCSA 600 °C 28 days	17,844	11,642	1,533
OPC/SCSA 600 °C 90 days	17,810	13,918	1,280
OPC/SCSA 700 °C 7 days	16,721	11,955	1,399
OPC/SCSA 700 °C 28 days	16,473	11,479	1,435
OPC/SCSA 700 °C 90 days	15,956	12,444	1,282
OPC/SCSA 800 °C 7 days	15,210	10,430	1,458
OPC/SCSA 800 °C 28 days	15,393	10,275	1,498
OPC/SCSA 800 °C 90 days	19,200	12,359	1,554
OPC/SCSA 900 °C 7 days	21,429	13,888	1,543
OPC/SCSA 900 °C 28 days	16,286	10,478	1,554
OPC/SCSA 900 °C 90 days	19,011	11,703	1,624

used. As in the case of the ashes, all green cement samples were analyzed at the X-ray powder diffraction D10B-XPD beamline of LNLS. In addition, the reaction between SCSAs and $Ca(OH)_2$ could be followed by XRD analysis of the specimens cured 7, 28, and 90 days.

The three-dimensional pore structure of the Portland green cements was obtained by laboratorial X-ray microtomography. The measurements were performed using an imaging setup of the HZB (Helmholtz Centre Berlin for Materials and Energy). This setup consisted a micro-focus 150 kV Hamamatsu X-ray source with a tungsten target and a flat panel detector C7942 ($120 \times 120\ mm^2$, $2240 \times 2368\ pixel^2$, pixel size of 50 μm). A 120 kV filament voltage and a current of 83 μA with an exposure time of 1.4 s per angular projection were used for the scan. The source-object distance was 250 mm and the source-detector distance was 550 mm, achieving thus a magnification factor of 2.2 which reflected in a voxel size of 4096 μm^3. During sample rotation, 1000 radiographic projection images were taken. The commercially available software Octopus V8.6 was used to perform the tomographic reconstruction which was based on a back-projection algorithm with convolution and correction for cone beam.

3. Results and discussion

3.1. Chemical and structural characterization of SCSAs

The chemical composition and loss on ignition (LOI) of the sugarcane ashes for the four calcination temperatures investigated here are summarized in Table 1. We observed that increasing the temperature tended to reduce the LOI. The SiO_2 content was over 60% of the inorganic matter. The other main components were Al_2O_3, K_2O, Fe_2O_3, CaO, and SO_3.

Fig. 1 shows the X-ray diffraction patterns of the four SCSAs obtained at different calcining temperatures, i.e., 600, 700, 800 and 900 °C. Rietveld analyzes of these diffraction patterns were performed to quantify the minerals found in the ashes afterwards. We could observe some striking similarities between all samples related to their mineralogical phases (Figs. 1 and 2). First, a large amount of quartz and amorphous structures could be identified in all diffraction patterns. The amorphicity of the SCSAs and some sharp diffraction peaks in the angular 2θ range of 20° to 30° could be clearly visualized, as shown in Fig. 2. The central halo around 22°2θ is related to the overlap of silica amorphous phases [21]. This amorphicity halo indicates the ash reactivity.

The particle size of the ashes was measure to assess the surface contact of each ash after grinding [18]. The results of the equivalent diameter and the surface area of the ashes are showed in the Table 2. The granulometric distribution of the ashes after grinding is showed in the Fig. 3.

Previous analysis of sugarcane ashes shows that material with D80 below 60 μm and a surface area above 30 m^2/kg are suitable to be used as pozzolanic material [18]. The ashes produced in all temperature burns meet these characteristics. The chemical and physical properties of ashes shows that all ashes studied in this work were suitable to be utilized as pozzolan. The sum of the oxides SiO_2, Al_2O_3 and Fe_2O_3 are higher than 50%, the SO3 content was below 5%. The XRD shows amorphicity and the granulometric distribution was adequate.

3.2. XRD analysis

The characterization of the OPC/SCSA green cements by synchrotron x-ray diffraction allowed a qualitative and quantitative study of crystalline phases by observing its fingerprints [16]. Thus, the diffractograms allowed identifying all the primary phases in the pure OPC (reference sample) and OPC/SCSA green cements such as Alite, Belite, Portlandite, Calcite, Ettringite, Brownmillerite and Periclase phases (Table 3). According to the literature, C_3S exhibits six polymorphs in the temperature range of room temperature to 1100 °C; we observed two C_3S polymorphs instead.

Portlandite could be detected in the diffractograms of the OPC and OPC/SCSA samples as result of the cement hydration (Fig. 1) while Quartz was present only in those cement samples which were partially replaced by SCSAs.

Although X-Ray diffraction is widely used in structural analysis of cementitious materials, quantify the amorphous phase has been always a difficult task because it depends on addition of internal standards. In this study, a different approach was done using a CSH phase as one of the mineral phases to refine the diffractograms in a Rietveld Analysis [30]. The Rietveld structure refinement method is able to distinguish overlapped peaks from distinct phases and quantify them [31–34]. This method was applied over the entire measure profile (10–80° 2theta) using the analytic software TOPAS [35].

Fig. 4 shows the refinements for the OPC and OPS/SCSA cured for 7 days. The refinement result was presented exhibiting the experimental and calculated data, and the difference between these values, in a single diagram. Also, the Bragg peaks of the phases considered to the refinement are showed below the graphs. Table 4 shows the Goodness of Fit (GOF) and the reliable factors of the Rietveld refinement (R_{exp} and R_{wp}), which are a way to evaluate if the Rietveld refinement was properly done.

Fig. 5 displays the quantitative Rietveld analysis results for the OPC and the several OPC/SCSA samples, for the main phases: C_3S, C_2S, CH, $CaCO_3$, CSH, and Ettringite. For the reference sample, all phases follow the same behavior as already presented by other authors [36].

In general, all green cements (OPC/SCSA samples) presented a strong dependence on the curing time. Comparing OPC/SCSA samples to the reference one, we could observe that alite(C_3S) and aluminate reacted faster than belite(C_2S) and browmillerite(C_4AF) (Fig. 5) [37]. The anhydrous phases, C_3S and C_2S, were consumed for all the samples (Fig. 6-a), what is a direct evidence of the formation of CH and CSH phases (Fig. 6-b,c) [36,37]. Moreover, OPC/SCSA-700 samples with 7 days of curing presented higher amount of C_3S than the other samples (OPC/SCSA-600 OPC/SCSA-800, OPC/SCSA-900) suggesting a delay in degradation of C_3S.

In accordance to the results concerned to the resistence to compression tests (Turkey method) [18] where OPC/SCSA-700 e OPC/SCSA-600 samples have shown similar behavior likewise the standard sample (at 29,69 MPa), there are strong evidences that the substitution of 20% in the cimentitious matrix by the sugarcane

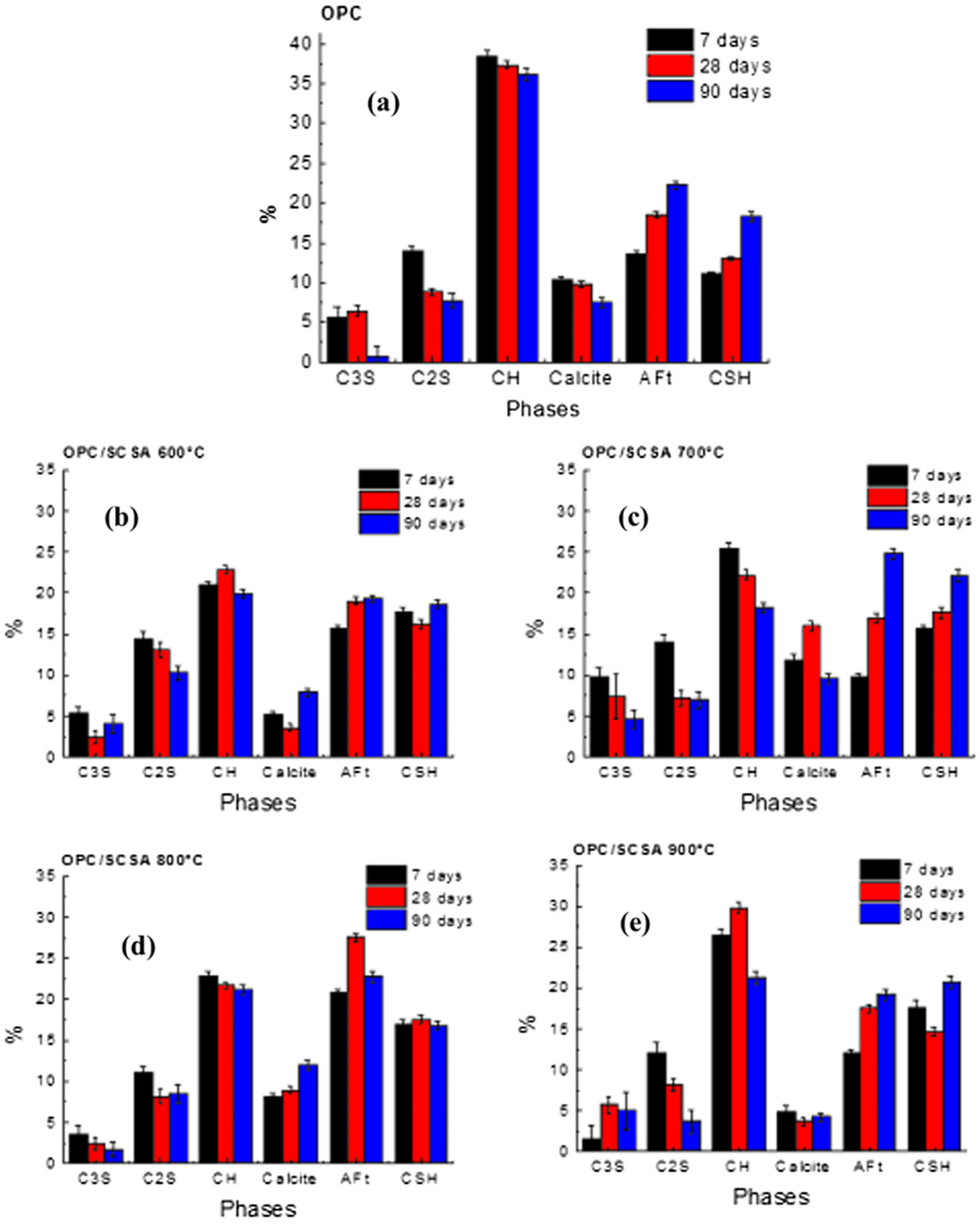

Fig. 5. Quantitative Rietveld analysis for OPC (a) and OPC/SCSA 600 (b); OPC/SCSA 700 (c),OPC/SCSA 800 (d); OPC/SCSA 900 (e).

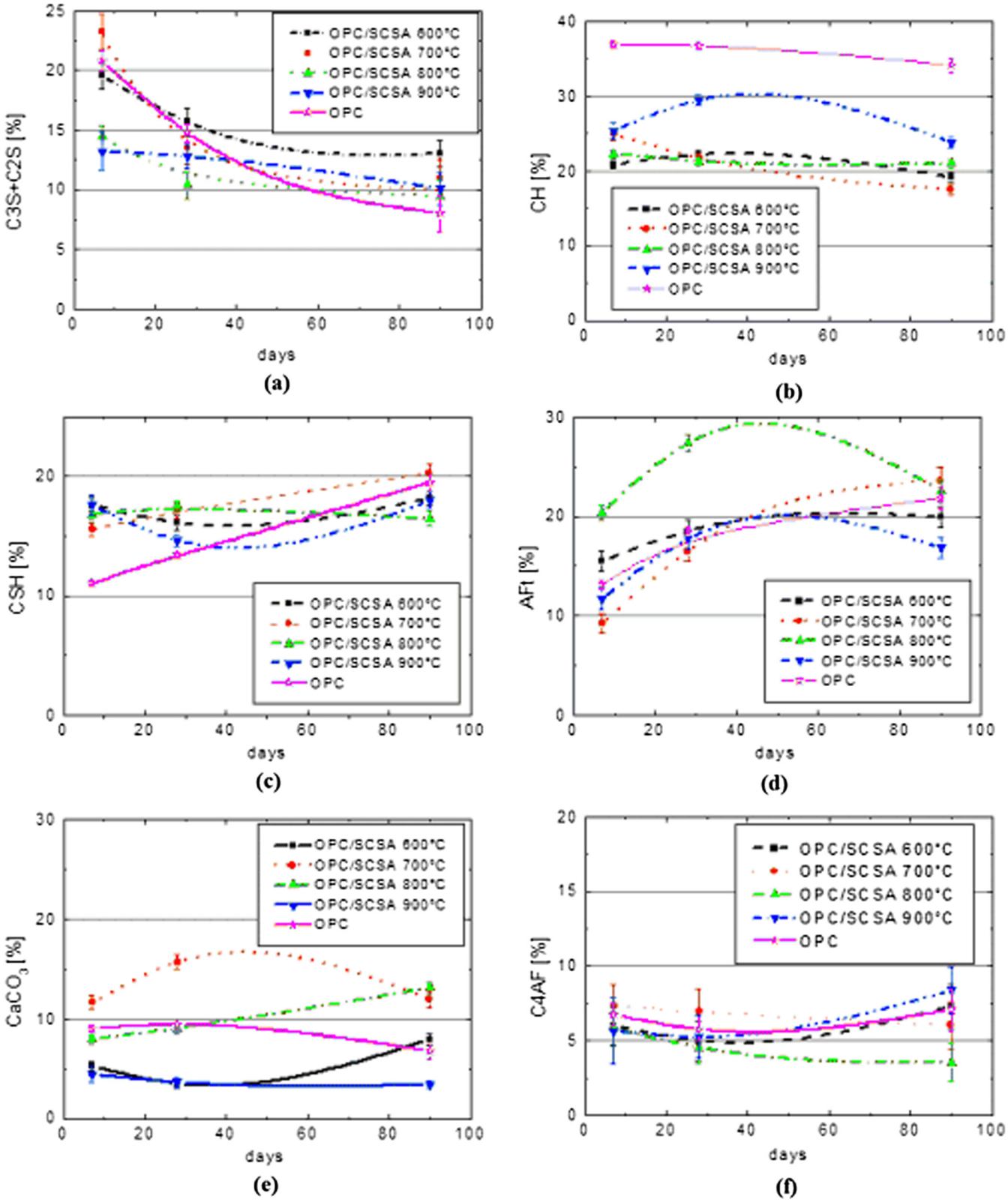

Fig. 6. Results of the Rietveld analysis for anhydrous phases C_3S and C_2S (a), Portlandite (b), CSH phase (c), Ettringite (d), Calcite (e), and Brownmillerite (f).

straw ashes can be used, without affecting the mechanical properties.

For the curing period of time of 7–28 days, the amount of anhydrous cement phases (C_3S and C_2S) for OPC/SCSA-600, OPC/SCSA-700, and OPC/SCSA-800 showed a decrease similar to the control sample (Fig. 6-a). On the order hand, the rate of the C_3S and C_2S reduction for OPC/SCSA-900 was much smaller than that of the reference sample (OPC). Specifically, the rate of reduction of the anhydrous cement phases for OPC/SCSA-600, OPC/SCSA-700, OPC/SCSA-800, and the reference sample are about

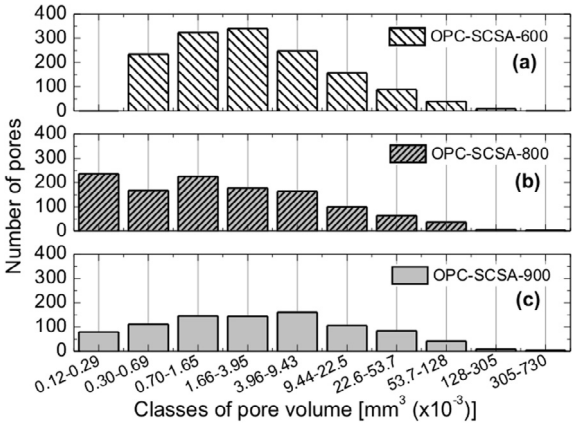

Fig. 7. Distribution of classes of pore volume to OPC/SCSA 600 (a); OPC/SCSA 800 (b), and OPC/SCSA 900 (c).

0.3% per day. For OPC/SCSA-900, this rate was approximately ten times slower. This suggests that green cements with ashes burned at 600, 700, and 800 °C exhibit higher reactivity than OPC/SCSA-900.

For the samples OPC/SCSA-700, OPC/SCSA-800, and the reference, in the period between 7 and 28 curing days, the CH degradation is related to the reaction of this phase with ash phases, producing calcite (Fig. 6-b,e). However, the tendency of CH, CSH, and $C_3S + C_2S$ phases during 28 and 90 curing days for all green cement samples was similar to the reference one.

In addition, OPC/SCSA-600 and OPC/SCSA-900 presented an increase in CH phase within 7 to 28 curing days, suggesting that ashes burned at these temperatures caused a delay in the degradation reaction of alite and belite. For 90 curing days all OPC/SCSA samples showed greater amount of alite and belite than the control, what pointed out that samples with ashes show less reactivity [37]. The C_3S and C_2S behavior as a function of curing time might be correlated with the amount of AFt, which exhibited a continuous increase in its amount except for OPC/SCSA-800 and OPC/SCSA-900 (Fig. 6-d). However, at the end of 90 days the quantity of AFt are greater than the amounts shown at 7 days of curing time, this implies that the reactions of hidration continued during the period of 7–90 days.

3.3. X-ray microtomography

Fig. 7 shows that the pore volumes distribution curves of samples OPC/SCSA-600 and OPC/SCSA-900 resemble a Gaussian with displaced center while for the SCSA-800 sample the curve starts in the middle of the Gaussian, i.e., has a larger number of smaller pores gradually decreasing until reaching the band from 0.10 to 0.25 mm^3. The histograms obtained from the reconstruction of the images showed that the OPC/SCSA-600 do not present pores in the range of 0.10–0.25 mm^3, whereas the OPC/SCSA-800 and OPC/SCSA-900 samples had pores in this range. This result could also be observed visually by images showed in Fig. 8.

Table 5 presents the total pore volume and the porosity of the SCSA-600, SCSA800, and SCSA-800 samples. It was possible to observe that the pores fraction in the samples increased for higher calcining temperatures.

Table 5
Pore volumes and pore fractions in the samples SCSA-600, SCSA-800, SCSA-900.

	SCSA600	SCSA800	SCSA900
Total pore volume[mm^3]	8.95	12.87	15.00
Sample volume[mm^3]	1338.37	1478.07	1289.70
Pore fraction[%]	0.65	0.87	1.17

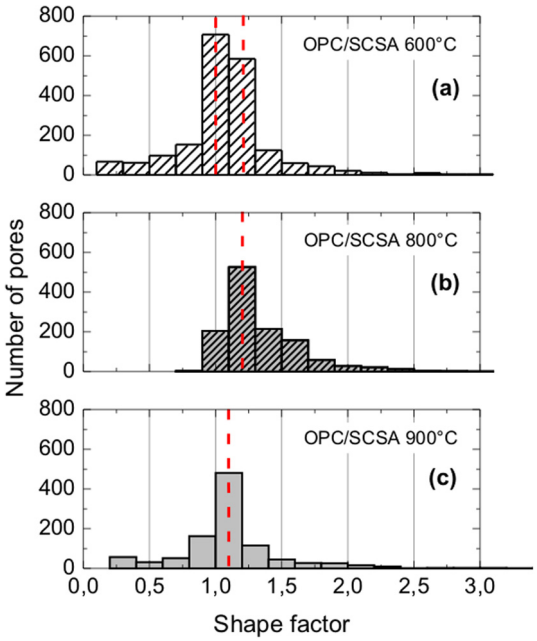

Fig. 9. OPC/SCSA-600 (a), OPC/SCSA-800 (b) and OPC/SCSA-900 (c).

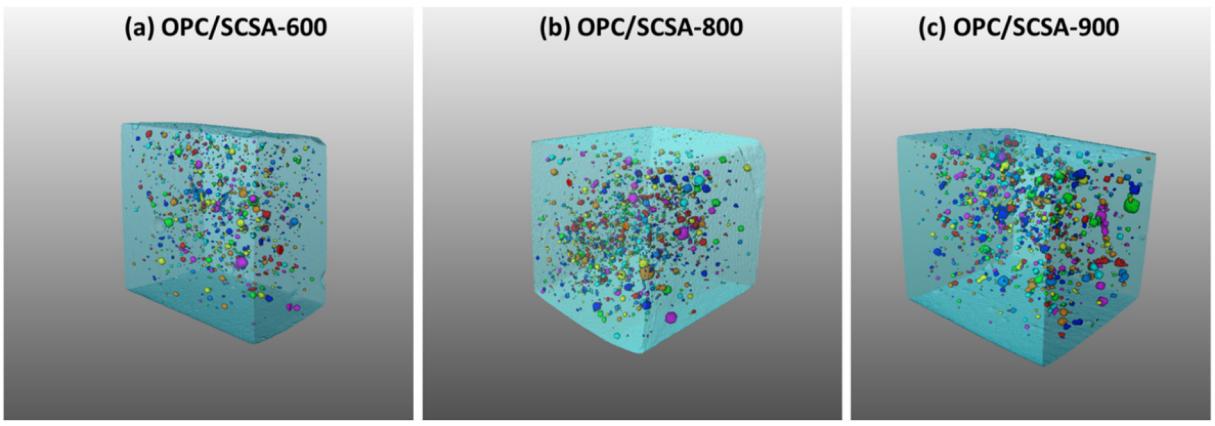

Fig. 8. Images of to OPC/SCSA 600 (a); OPC/SCSA 800 (b) and OPC/SCSA 900 (c).

Another parameter analyzed was the Shape Factor of the pores, which takes into account the surface area of voids and the area of the smaller cross-section that passes through the center of mass according to the equation below:

$$\text{Form Factor} = \frac{(\text{surface area})^3}{36 \cdot \pi \cdot (\text{cross} - \text{section area})^2}$$

This parameter equals 1 when a pore has a spherical shape. As this factor increases, the shapes of the pore approach to an ellipsoid.

Fig. 9 showed by distribution of the shape factor that OPC/SCSA-600 and OPC/SCSA-900 present porous with prevalence spherical. On other hand, OPC/SCSA-800 has porous shape slightly ellipsoid.

4. Conclusions

In order to minimize the environmental and social impacts engendered in the cement production, the present study aimed to investigate the substitution of cement by the sugar cane straw ashes produced by controlled burning, as a mineral addition in cementitious matrix, thus assessing its perspective in industrial applicability. The sugar cane straw were submitted to four different burning temperatures: 600, 700, 800, 900 °C. The results show that the adopted procedure to produce the ashes were considered efficient, i. e., a pre-burning at 400 °C for 20 min and temperature thresholds at 600, 700, 800 or 900 °C for 1 h, enable the obtainment of reactive ashes. Physical characterizations of the burning ashes, using granulometric distribution and X-ray powder diffraction, demonstrate that part of the material is amorphous, indicating a prospective to be considered pozzolans.

Glimpsing the way to sustainability, the idea of introducing agroindustrial wastes, as sugar cane ashes into the Ordinary Portland Cement, opens a wide field of applicability. Therefore, it is necessary to know its behavior according to the mineralogical variability. Based on characterization results of the samples of sugarcane bagasse ash, it can be concluded that:

Using the association of the synchrotron radiation X-ray powder diffraction and Rietveld refinement method we observed the existence of the main compounds: Alite, Belite, Portlandite, Ettringite, Calcite, and Brownmillenite into OPC and OPC/SCSA. Emphasize that in addition to the crystalline phases also was considered the amorphous component. The well-known C-S-H was taken into account in the analyses.

The tomography characterization, carried out after 90 days indicated that the folders with the ashes SCSA-600 had lower volumes of pores and capillary pores smaller among the evaluated folders. It was possible that the use of different thermally treated sugar cane straw ashes induce the formation of pores with different size and form. Furthermore, we note the changing in the amount of pores.

The results obtained in this study indicate that the replacement of 20% of the clinker by the SCSA, shows to be a good option to recover the agroindustrial wastes. Finally, the results presented in this study indicate that the OPC/SCSA-700 sample shows similar quality to control sample.

References

[1] IEA, IEA, Int. Energy Agency – IEA Glob. Energy-Relat.Emiss. Carbon Dioxide Stalled 2014. http://www.iea.org/newsroomandevents/news/2015/march/global-energy-related-emissions-of-carbon-dioxide-stalled-in-2014.html (accessed June 6, 2016).

[2] T.A. Boden, G. Marland, R.J. Andres, Global, Regional, and National Fossil-Fuel CO_2 Emissions, 2010. http://cdiac.ornl.gov/trends/emis/overview_2007.html (accessed June 6, 2016).

[3] CONAB, Conab, Conab – Cia. Nac.Abast. (2012). http://www.conab.gov.br/ (accessed June 6, 2016).

[4] J. Martirena Hernández, B. Middendorf, M. Gehrke, H. Budelmann, Use of wastes of the sugar industry as pozzolana in lime-pozzolana binders: study of the reaction, Cem. Concr. Res. 28 (1998) 1525–1536, http://dx.doi.org/10.1016/S0008-8846(98)00130-6.

[5] S.K. Malhotra, N.G. Dave, Investigations into the effect of addition of flyash and burnt clay pozzolana on certain engineering properties of cement composites, Cem. Concr. Compos. 21 (1999) 285–291, http://dx.doi.org/10.1016/S0958-9465(99)00006-2.

[6] F. Martirena, B. Middendorf, R.L. Day, M. Gehrke, P. Roque, L. Martínez, S. Betancourt, Rudimentary, low tech incinerators as a means to produce reactive pozzolan out of sugarcane straw, Cem. Concr. Res. 36 (2006) 1056–1061, http://dx.doi.org/10.1016/j.cemconres.2006.03.016.

[7] J. Payá, J. Monzó, M.V. Borrachero, L. Díaz-Pinzón, L.M. Ordóñez, Sugar-cane bagasse ash (SCBA): studies on its properties for reusing in concrete production, J. Chem. Technol. Biotechnol. 77 (2002) 321–325, http://dx.doi.org/10.1002/jctb.549.

[8] V.N. Dwivedia, N.P. Singhb, S.S. Dasa, N.B. Singha, A new pozzolanic material for cement industry: bamboo leaf ash, Int. J. Phys. Sci. 1 (2006) 106–111.

[9] M. Frìas, M.I.S. de Rojas, J. Cabrera, The effect that the pozzolanic reaction of metakaolin has on the heat evolution in metakaolin-cement mortars, Cem. Concr. Res. 30 (2000) 209–216. 00231-8.

[10] M. Frías, E. Villar-Cociña, E. Valencia-Morales, Characterisation of sugarcane straw waste as pozzolanic material for construction: calcining temperature and kinetic parameters, Waste Manage. 27 (2007) 533–538, http://dx.doi.org/10.1016/j.wasman.2006.02.017.

[11] L.J. Parrott, M. Geiker, W.A. Gutteridge, D. Killoh, Monitoring Portland cement hydration: comparison of methods, Cem. Concr. Res. 20 (1990) 919–926, http://dx.doi.org/10.1016/0008-8846(90)90054-2.

[12] M.F. Rojas, M.I. Sánchez de Rojas, Influence of metastable hydrated phases on the pore size distribution and degree of hydration of MK-blended cements cured at 60 °C, Cem. Concr. Res. 35 (2005) 1292–1298, http://dx.doi.org/10.1016/j.cemconres.2004.10.038.

[13] F. Ridi, E. Fratini, P. Baglioni, Cement: a two thousand year old nano-colloid, J. Colloid Interface Sci. 357 (2011) 255–264, http://dx.doi.org/10.1016/j.jcis.2011.02.026.

[14] ABNT, High early strength Portland cement, Brazilian Technical Standard Association, Rio de Janeiro, 1991.

[15] ASTM, Standard specification for coal fly ash and raw or calcined natural pozzolan for use in, concrete, American Society for Testing and Materials, Philadelphia, 2003.

[16] F.F. Ferreira, E. Granado, W. Carvalho Jr., S.W. Kycia, D. Bruno, R. DroppaJr, X-ray powder diffraction beamline at D10B of LNLS: application to the Ba_2FeReO_6 double perovskite, J. Synchrotron Radiat. 13 (2006) 46–53, http://dx.doi.org/10.1107/S0909049505039208.

[17] C. Cusatis, M. Kobayashi Franco, E. Kakuno, C. Giles, S. Morelhão, V. Mello, I. Mazzaro, A versatile X-ray diffraction station at LNLS (Brazil), J. Synchrotron Radiat. 5 (1998) 491–493, http://dx.doi.org/10.1107/S0909049598000685.

[18] M.S. Rodrigues, Avaliação de Cinzas de Palha de Cana-De-Açúcar e sua Utilização Como Adição Mineral em Matrizes Cimentícias, Tese – Doutorado, Universidade Estadual de Campinas, 2012.

[19] Á.G. De La Torre, S. Bruque, J. Campo, M.A.G. Aranda, The superstructure of C3S from synchrotron and neutron powder diffraction and its role in quantitative phase analyses, Cem. Concr. Res. 32 (2002) 1347–1356, http://dx.doi.org/10.1016/S0008-8846(02)00796-2.

[20] V.K. Peterson, B.A. Hunter, A. Ray, Tricalcium silicate T1 and T2 polymorphic investigations: rietveld refinement at various temperatures using synchrotron powder diffraction, J. Am. Ceram. Soc. 87 (2004) 1625–1634, http://dx.doi.org/10.1111/j.1551-2916.2004.01625.x.

[21] M.G. Silva, Cimentos Portland com adições minerais, Mater. Constr. Civ. E Princípios Ciênc. E Eng. Mater. São Paulo IBRACON. 1 (2007) 761–793.

[22] M.-N. deNoirfontaine, M. Courtial, F. Dunstetter, G. Gasecki, M. Signes-Frehel, Tricalcium silicate Ca_3SiO_5 superstructure analysis: a route towards the structure of the M1 polymorph, Z. FürKrist. Cryst. Mater. 227 (2011) 102–112, http://dx.doi.org/10.1524/zkri.2012.1425.

[23] W. Mumme, R. Hill, G. Bushnell-Wye, E. Segnit, Rietveld crystal structure refinements, crystal chemistry and calculated powder diffraction data for the polymorphs of dicalcium silicate and related phases, NeuesJahrb Miner. Abh. 169 (1995).

[24] D.M. Henderson, H.S. Gutowsky, A nuclear magnetic resonance determination of the hydrogen positions in $Ca(OH)_2$, 1962.

[25] F. Goetz-Neunhoeffer, J. Neubauer, Refined ettringite ($Ca_6Al_2(SO_4)_3(OH)_{12}\cdot 26H_2O$) structure for quantitative X-ray diffraction analysis, Powder Diffr. 21 (2006) 4–11, http://dx.doi.org/10.1154/1.2146207.

[26] H. Sitepu, B.H. O'Connor, D. Li, Comparative evaluation of the March and generalized spherical harmonic preferred orientation models using X-ray diffraction data for molybdite and calcite powders, J. Appl. Crystallogr. 38 (2005) 158–167, http://dx.doi.org/10.1107/S0021889804031231.

[27] A.A. Colville, S. Geller, The crystal structure of brownmillerite, Ca_2FeAlO_5, Acta Crystallogr. B 27 (1971) 2311–2315, http://dx.doi.org/10.1107/S056774087100579X.

[28] S. Sasaki, K. Fujino, Y. Takéuch, X-ray determination of electron-density distributions in oxides, MgO, MnO, CoO, and NiO, and atomic scattering factors of their constituent atoms, Proc. Jpn. Acad. Ser B Phys. Biol. Sci. 55 (1979) 43–48.

[29] S.M. Antao, I. Hassan, J. Wang, P.L. Lee, B.H. Toby, State-of-the-art high-resolution powder X-ray diffraction (HRPXRD) illustrated with Rietveld structure refinement of quartz, sodalite, tremolite, and meionite, Can. Mineral. 46 (2008) 1501–1509.

[30] S.T. Bergold, F. Goetz-Neunhoeffer, J. Neubauer, Quantitative analysis of C–S–H in hydrating alite pastes by in-situ XRD, Cem. Concr. Res. 53 (2013) 119–126, http://dx.doi.org/10.1016/j.cemconres.2013.06.001.
[31] H. Rietveld, A profile refinement method for nuclear and magnetic structures, J. Appl. Crystallogr. 2 (1969) 65–71.
[32] M. Paul, Application of the Rietveld method in the cement industry, Microstruct. Anal.Mater. Sci. Freib. Ger. (2005).
[33] G. Le Saoût, V. Kocaba, K. Scrivener, Application of the Rietveld method to the analysis of anhydrous cement, Cem. Concr. Res. 41 (2011) 133–148.
[34] F. Guirado, S. Galı, S. Chinchón, Quantitative Rietveld analysis of aluminous cement clinker phases, Cem. Concr. Res. 30 (2000) 1023–1029.
[35] A.A. Coelho, J. Evans, I. Evans, A. Kern, S. Parsons, The TOPAS symbolic computation system, Powder Diffr. 26 (2011) S22–S25.
[36] G.A. Calligaris, M.K.K.D. Franco, L.P. Aldrige, M.S. Rodrigues, A.L. Beraldo, F. Yokaichiya, X. Turrillas, L.P. Cardoso, Assessing the pozzolanic activity of cements with added sugarcane straw ash by synchrotron X-ray diffraction and Rietveld analysis, Constr. Build. Mater. 98 (2015) 44–50, http://dx.doi.org/10.1016/j.conbuildmat.2015.08.103.
[37] H.F.W. Taylor, Cement Chemistry, Academic Press, London, 1990.